

Quantum Simulation of the Haldane Phase Using Trapped Ions

I. Cohen¹ and A. Retzker¹

¹*Racah Institute of Physics, The Hebrew University of Jerusalem, Jerusalem 91904, Givat Ram, Israel*

(Dated: February 28, 2024)

A proposal to use trapped ions to simulate spin-one XXZ antiferromagnetic (AFM) chains as an experimental tool to explore the Haldane phase is presented. We explain how to reach the Haldane phase adiabatically, demonstrate the robustness of the ground states to noise in the magnetic field and Rabi frequencies, and propose a way to detect them using their characterizations: an excitation gap and exponentially decaying correlations, a nonvanishing nonlocal string order and a double degenerate entanglement spectrum. Scaling up to higher dimensions and more frustrated lattices, we obtain richer phase diagrams, and we can reach spin liquid phase, which can be detected by its entanglement entropy which obeys the boundary law.

PACS numbers: 03.67.Ac, 03.67.-a, 37.10.Vz

Quantum simulation[1, 2] is a promising direction for the exploration of many-body physics. Many different experimental platforms have been designed to conduct quantum simulation experiments, ranging from cold atomic gases in optical lattices[3, 4], trapped ions[5], cavity QED [6–8], superconducting circuits[9] to linear optics[10]. The simulation of spin chains has attracted special attention [9, 11–14]. In particular trapped ions have been targeted as a promising system for the realization of spin chain Hamiltonians[15, 16]. Theoretical proposals [17, 18] have also triggered experimental work [19–23].

In the last three decades, a great deal of theoretical effort has been invested in understanding the physics of one dimensional one-spin AFM Heisenberg chains; namely, the Haldane phase. According to Haldane’s conjecture [24] integer-spin AFM Heisenberg chains, as described by the following Hamiltonian

$$H = \sum_i S_x^i S_x^{i+1} + S_y^i S_y^{i+1} + \lambda S_z^i S_z^{i+1} + D (S_z^i)^2 \quad (1)$$

will have short range correlation functions, and a finite gap between the ground and excited states. In contrast, half-integer spin chains will have long-range correlations and will be gapless. Kennedy and Tasaki [25, 26] showed that the Haldane phase is related to the breaking of a hidden $Z_2 \times Z_2$ symmetry that is introduced by a non-local unitary transformation, and followed by a nonzero, nonlocal string order parameter. Recently, Oshikawa *et al.* [27, 28] showed that in the most general case, the Haldane phase can be defined by a symmetry-protected double-degeneracy, even if the string order and the gapless edge states are absent. We take advantage of these qualities of Haldane phase to form the Hamiltonian adiabatically and to measure its ground states.

In what follows, we propose a scheme to simulate spin one XXZ AFM systems. To the best of our knowledge, there is no experimentally convenient system for exploring the Haldane phase or higher dimensional integer-spin Heisenberg AFM systems. Complicated experiments using neutron scattering from a one-spin AFM Heisenberg chain CsNiCl_3 have measured the excitation spectrum and found an energy gap [30]. However, a trapped ions platform for the quantum simulation

of the Haldane phase, enables much more to be said and examined, in a much more experimentally feasible way.

The model — In our model we have N ions of mass m and charge e , in a linear trap with frequencies $\omega_x, \omega_y, \omega_z$. The MHz trap frequencies are tunable so as to construct the desired geometric shape of the ion lattice. A Coulomb interaction causes the trapped ions to vibrate around fixed points $r_{i\alpha} = r_{i\alpha}^0 + \Delta r_{i\alpha}$ of the i^{th} ion in the α direction, whose geometric formation is determined by the equilibrium between the trapping forces and the Coulomb repulsion. In the harmonic approximation the vibration Hamiltonian [31, 32] is

$$H_{\text{vib}} = \sum_{i,\alpha} \left(\frac{1}{2m} p_{i,\alpha}^2 + \frac{1}{2} m \omega_\alpha^2 \Delta r_{i,\alpha}^2 \right) + \frac{e^2}{2} \sum_{i,j,\alpha,\beta} V_{ij\alpha\beta} \Delta r_{i\alpha} \Delta r_{j\beta} \quad (2)$$

By solving the quadratic problem we obtain the normal modes of the vibration (Fig. 1) $M_{i,n}^\alpha$ and v_n^α which are the eigenstates and the eigenvalues of the n^{th} mode and the i^{th} ion in α direction respectively. Thus, the ion displacements are represented by these normal modes as $\Delta r_{i\alpha} = \sum_n M_{i,n}^\alpha \sqrt{2m v_n^\alpha} (b_{n\alpha}^\dagger + b_{n\alpha})$, while the vibration Hamiltonian becomes

$$H_{\text{vib}} = \sum_{n,\alpha} v_n^\alpha b_{n\alpha}^\dagger b_{n\alpha}. \quad (3)$$

The proposed scheme concentrates on the microwave quantum computing setup [18, 33, 34] where the spin degrees of freedom are modelled via the hyperfine structure (Fig. 2 left). The energy levels configuration is produced by the $F=0$ singlet state $|0\rangle$ and the triplet $F=1$ states $|-1\rangle, |0'\rangle$ and $|1\rangle$ according to their spin projection on the z direction. Two resonant microwave fields with the same Rabi frequency Ω drive the transitions $|\pm 1\rangle \longleftrightarrow |0\rangle$. According to their relative phases, the dressed states, which will play the role of the simulated $S=1$ spins, are obtained. For the vanishing initial phase difference, the dressed state basis is the eigenvector set of F_x (the projection of the hyperfine spin on the x axis), and is expanded by the original basis $\{|1\rangle, |0\rangle, |-1\rangle\}$ as the following: $|u\rangle = \frac{1}{\sqrt{2}} \left(\frac{|1\rangle + |-1\rangle}{\sqrt{2}} + |0\rangle \right)$, $|D\rangle = \frac{-|1\rangle + |-1\rangle}{\sqrt{2}}$,

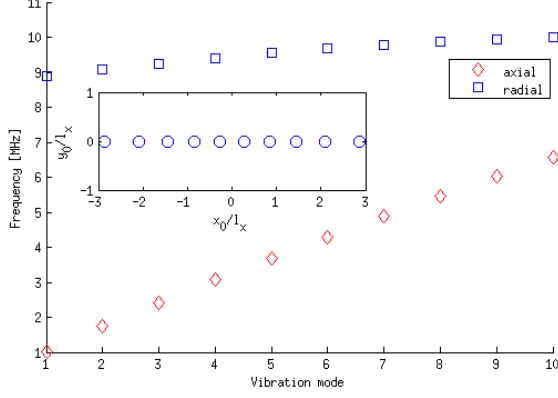


Figure 1. **Vibration modes.** Radial and axial vibration frequencies for $N=10$ trapped ions in a linear formation (legend) calculated when the trap frequencies are $\omega_x = 1\text{MHz}$ $\omega_y = 10\text{MHz}$. The inset shows the equilibrium positions of the ions.

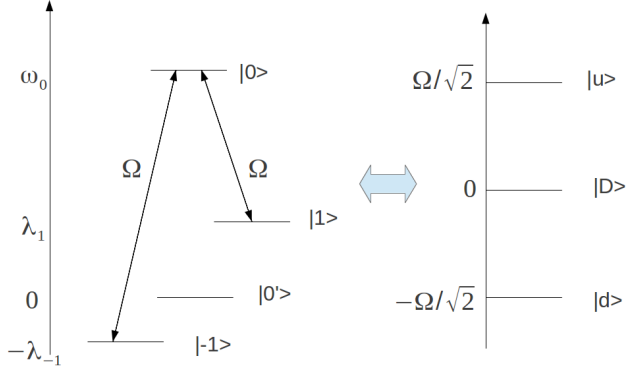


Figure 2. **Spin Energy levels.** Hyperfine energy levels and the driving fields (left side) that are used for preparing the effective Hamiltonian H_{XY} in the dressed state basis (right side).

$|d\rangle = \frac{1}{\sqrt{2}} \left(\frac{|1\rangle + |-1\rangle}{\sqrt{2}} - |0\rangle \right)$, with the eigenvalues $\frac{\Omega}{\sqrt{2}}, 0, -\frac{\Omega}{\sqrt{2}}$ respectively (Fig. 2 right).

To induce the spin-spin interaction which is achieved by the creation of a virtual phonon in one ion and its annihilation in another ion, there should be a term in the Hamiltonian that couples the spin and the vibration. Therefore, the very small Lamd-Dicke parameter of microwave sources requires the use of large and stable magnetic field gradients [18, 35] where the field is polarized in the z direction, resulting in adding the term $g\mu_B F_z^i \partial_\alpha B_z \Delta r_{i,\alpha}$, where g is the Lande g -factor and μ_B is the Bohr magneton. In the interaction picture according to the hyperfine structure, the Hamiltonian has the form of

$$H_I = \sum_{i,n,\alpha} \frac{\Omega}{\sqrt{2}} F_x^i + v_n^\alpha (b_{n\alpha}^\dagger b_{n\alpha} + \eta_{in}^\alpha (b_{n\alpha}^\dagger + b_{n\alpha}) F_z^i) \quad (4)$$

where $\eta_{in}^\alpha = \frac{g\mu_B \partial_\alpha B_z M_{i,n}^\alpha}{\sqrt{2} m v_n^\alpha} \ll 1$.

To manifest the coupling of the phonons to the spins a polaron-like transformation is performed $U_P = e^{-P}$, $P =$

$-\sum_{n,i,\alpha} \frac{\eta_{in}^\alpha F_z^i}{v_n^\alpha} (b_{n\alpha}^\dagger - b_{n\alpha})$. After transforming to the interaction picture according to the carrier transition $\frac{\Omega}{\sqrt{2}} F_x$ and the vibration Hamiltonian (Eq. 3), the spin-dependent force in the dressed basis is obtained:

$$H_I = \frac{\Omega}{2\sqrt{2}} \sum_{n,i,\alpha} \eta_{in}^\alpha \left(S_+^i e^{i\frac{\Omega}{\sqrt{2}}t} - S_-^i e^{-i\frac{\Omega}{\sqrt{2}}t} \right) (b_{n\alpha}^\dagger e^{i v_n^\alpha t} - b_{n\alpha} e^{-i v_n^\alpha t}) \quad (5)$$

Expanding the Dyson series of the time propagator to the second order in H_I we obtain two terms in the Hamiltonian $H_{eff} = H_{res} + H_{XY}$:

$$H_{res} = \sum_{j,n,m,\alpha,\beta} J_{jnm,\alpha\beta}^{res} S_z^j \left(b_{n\alpha}^\dagger b_{m\beta} + \frac{1}{2} \delta_{\alpha,\beta} \delta_{n,m} \right) e^{-i(v_n^\alpha - v_m^\beta)t} \quad (6)$$

$$H_{XY} = \sum_{i,j} J_{ij}^{eff} \left((S_x^i S_x^j + S_y^i S_y^j) (1 - \delta_{i,j}) - \frac{(S_z^j)^2}{2} \delta_{i,j} \right) \quad (7)$$

where

$$J_{jnm}^{res} = \sqrt{2}\Omega \left(\frac{\Omega}{4} \right)^2 \eta_{jn}^\alpha \eta_{jm}^\beta \left(\frac{1}{\left(\frac{\Omega}{\sqrt{2}} \right)^2 - (v_n^\alpha)^2} + \frac{1}{\left(\frac{\Omega}{\sqrt{2}} \right)^2 - (v_m^\beta)^2} \right) \quad (8)$$

$$J_{ij}^{eff} = \left(\frac{\Omega}{2} \right)^2 \sum_{n,\alpha} \eta_{in}^\alpha \eta_{jn}^\alpha \frac{2v_n^\alpha}{\left(\frac{\Omega}{\sqrt{2}} \right)^2 - (v_n^\alpha)^2} \propto |\vec{r}_i^0 - \vec{r}_j^0|_{i \neq j}^{-\alpha} \quad (9)$$

which gives the power-law spin-spin interactions, instead of the theoretical simplification of nearest neighbors interactions [17]. Although a constant D term, like the last term in Eq. 1, was obtained, we would like to pursue a tunable D coefficient. As we will see later in this article our model can be decoupled from H_{res} since its ground states belong to the decoherence-free subspace.

Generation of the anisotropy D term — Generating a tunable D term is achieved by applying an A.C. Stark shift using an additional microwave field corresponding to the transition between the states $|0'\rangle \longleftrightarrow |0\rangle$ with a red detuning Δ_r (Fig. 3 left). In the dressed-state basis $|0\rangle$ is transformed to $\frac{1}{\sqrt{2}}(|u\rangle - |d\rangle)$, therefore by moving to the interaction picture according to the carrier transition $\frac{\Omega}{\sqrt{2}} S_z$ as was mentioned above, which is followed by an expansion of Dyson series of the time propagator to the second order, all the off-diagonal terms are suppressed using the rotating wave approximation (RWA), if we assume that $\frac{\Omega_r}{2\sqrt{2}} \ll \frac{\Omega}{\sqrt{2}} \ll \Delta_r$. As a consequence, the anisotropy $D' = \frac{\Omega_r^2}{8\Delta_r}$ term is obtained, which is slightly different from D since the model is θ rotated while generating λ term.

Generation of the Ising-like λ term — Instead of producing the Ising-like anisotropy term $\lambda S_z^i S_z^{i+1}$ explicitly as was done with the anisotropy D term, we will use the following

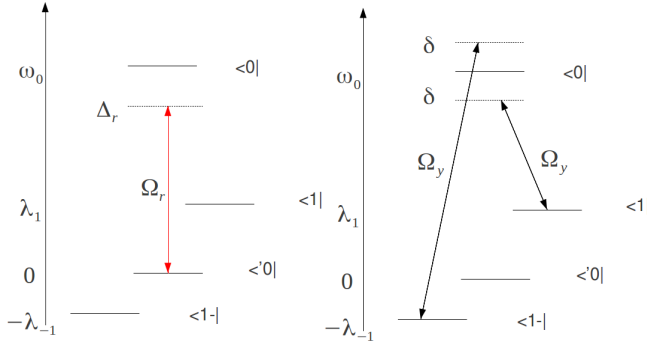


Figure 3. **Driving fields for creating the D and λ coefficients.** Left side: Generating the D term in Eq. 1 is done by an A.C. Stark shift via the red detuned Δ_r transition. Right side: The transitions that are required for generating $\Omega' S_y \sin \theta$ and applying the “trick” where $\delta = \left(\frac{\Omega}{\sqrt{2}} - \Omega' \cos \theta\right)$ is the detuning, $\pm \frac{\pi}{2}$ are the initial phases and $\Omega_y = \sqrt{2}\Omega' \sin \theta$ is the Rabi frequency.

“trick”. We will add $H_2 = \Omega' S_{z,\theta} = \Omega' (S_z \cos \theta - S_y \sin \theta)$ to the Hamiltonian, which is $\Omega' F_{x,\theta} = \Omega' (F_x \cos \theta - F_y \sin \theta)$ in the original basis. This is done by generating each term separately. The first term $\Omega' F_x \cos \theta = \Omega' S_z \cos \theta$ can be set aside from the previous microwave transitions that produce H_{XY} . The second term $\Omega' S_y \sin \theta$ (Fig. 3 right) is produced by applying two microwave fields corresponding to the transitions $|\mp 1\rangle \longleftrightarrow |0\rangle$ with $\pm \left(\frac{\Omega}{\sqrt{2}} - \Omega' \cos \theta\right)$ detunings, $\pm \frac{\pi}{2}$ initial phases and the same Rabi frequency $\sqrt{2}\Omega' \sin \theta$ respectively, after transforming to the interaction picture according to $\left(\frac{\Omega}{\sqrt{2}} - \Omega' \cos \theta\right) F_x$, and neglecting the fast rotating terms. The Rabi frequency should be much smaller than the original Rabi frequency namely $\Omega' \ll \Omega$, so the undesired spin to vibration coupling caused by the polaron-like transformation will be negligible. By applying a θ rotation around the x axis, the operators are transformed as follows: $S_{z,\theta} \rightarrow S_z$, $S_z \rightarrow S_z \cos \theta + S_y \sin \theta$, $S_y \rightarrow S_y \cos \theta - S_z \sin \theta$ and S_x is not changed, and the new dressed-state basis is θ rotated around the x axis as well. If we move to the interaction picture corresponding to the new term we have built and use RWA where we want $\frac{\eta_{in}\Omega}{2\sqrt{2}} \ll \Omega'$ we will end up with the following effective Hamiltonian

$$H_{eff} = \sum_{i \neq j} J_{ij}^{eff} \left\{ (S_x^i S_x^j + S_y^i S_y^j) \left(\frac{1 + \cos^2 \theta}{2} \right) + S_z^i S_z^j \frac{\sin^2 \theta}{2} \right\} + \sum_i \left(\frac{\Omega_r^2}{8\Delta_r} - \frac{J_{ii}^{eff}}{2} \right) \left(\frac{1 + \cos^2 \theta}{2} - \sin^2 \theta \right) (S_z^i)^2 \quad (10)$$

which is a one-spin XXZ AFM Hamiltonian with power-law spin-spin interactions. In Fig. 4 we illustrate the comparison between the Hamiltonian of the spin dependent force H_{Int} (Eq. 5, to which were added all the previous steps (Fig. 3)) and the effective Hamiltonian H_{eff} for two trapped ions, us-

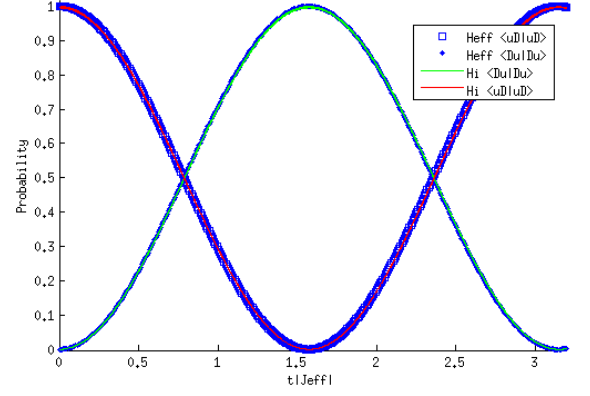


Figure 4. **Dynamics of two trapped ions for an initial state $|uD\rangle$** The probability of finding the system in states $|uD\rangle$ and $|Du\rangle$ calculated by both H_{eff} and H_{Int} , using the following physical values: $\eta = 0.03$, $v = 4\text{MHz}$, $\Omega = 6\sqrt{2}v$, $\theta = 1.47 \sim \frac{\pi}{2}$, $\Omega' = 0.6v$ (Rabi frequency of $S_{z,\theta}$ for the trick), $D' = -18.5\text{KHz}$ (the coefficient of S_z^2 obtained by the A.C Stark shift). We obtain the Haldane Hamiltonian with: $J_{eff} = 1.85\text{KHz}$ D coefficient $D = 4.35$ and λ coefficient $\lambda = 0.989$. This confirms that Eq. 10 was obtained appropriately.

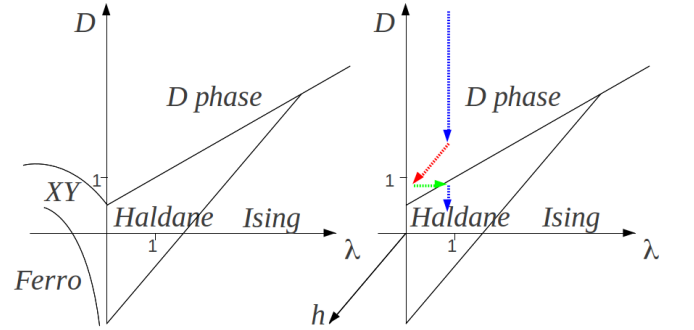


Figure 5. **Phase diagram and adiabatic path** Phase diagram of the Haldane phase, where the phases are the large D phase, the Haldane phase, the Ising-like phase, the XY phase and the ferromagnetic phase. The colored arrows represent the adiabatic path from the large D phase to Haldane phase. The blue arrow stands for lowering D coefficient, the red arrow stands for switching on the symmetry breaking h term while still lowering D and the green arrow stands for switching off the h term while lowering D .

ing physically reasonable values.

Reaching the Haldane phase adiabatically — In order to prepare the system in the Haldane phase and to reach its ground state, we first start with the large D Hamiltonian and generate its ground topologically trivial state which is a tensor product of local $|D\rangle$ states in every site [18, 34]. Then we switch on the required Hamiltonian adiabatically (*i.e.* slower than the energy gap) by lowering the D coefficient. For an infinite chain, a problem arises when we reach a second order phase transition in the phase diagram (Fig. 5) where the energy gap closes [36] and the adiabatic approximation cannot hold. To overcome this obstacle we take advantage of the fact that the Haldane phase is asymmetry-protected topolog-

ical phase. Far enough from the $D \rightarrow H$ phase transition we will adiabatically turn on a perturbation in the Hamiltonian that breaks all the symmetries in this system. Then, when we are in the region of the Haldane phase we will adiabatically turn this perturbation off. In that way we will not cross any second order phase border, and hence we will always stay in the adiabatic approximation.

The Haldane phase is protected by the following symmetries: a bond centered spatial inversion $\vec{S}_j \rightarrow \vec{S}_{-j+1}$, a time reversal symmetry $\vec{S}_j \rightarrow -\vec{S}_j$ or the dihedral D_2 symmetry which is the π rotations around x, y and z axes. In order to break all these symmetries we add a perturbation term $H_{\text{pert}} = -\hbar \sum_i (-1)^i S_z^i$. This term can be produced by individual addressing [35] using a microwave frequency comb with a staggered phase. Taking advantage of the magnetic field gradient along the chain axis, each ion experiences a different Zeeman splitting and only the right frequency from the comb can interact with it.

Before crossing the phase transition, the symmetry breaking perturbation should be turned on adiabatically, while still lowering the D coefficient in the Hamiltonian. Then, the perturbation should be turned off adiabatically, reaching the plane $h=0$ in the Haldane phase domain. If the time duration of this procedure is shorter than the coherence time, the ground state in the Haldane phase should be achieved with high fidelity.

Detecting and measuring the ground states — As a topological phase, the Haldane phase does not obey the Landau paradigm and cannot be characterized by a local order parameter. However there are other properties that can characterize it: 1) an excitation gap and exponentially decaying correlations $C_{ij}^\alpha = \langle S_i^\alpha S_j^\alpha \rangle - \langle S_i^\alpha \rangle^2$, 2) a nonvanishing nonlocal string order $O_{\text{string}}^\alpha(H) = \lim_{|i-j| \rightarrow \infty} \langle -S_i^\alpha \exp[i\pi \sum_{l=i+1}^{j-1} S_l^\alpha] S_j^\alpha \rangle$, where $\langle \rangle$ denotes the expectation value in the ground state, 3) a double degenerate entanglement spectrum, obtained by dividing the systems into two parts, tracing out one of them and diagonalizing the reduced density matrix [37].

Using trapped ions as a platform for quantum simulations allows us measure every spin state with high fidelity and accuracy. The tomography of an exponentially growing Hilbert space with the size of the system is time-consuming. Yet, efficient tailored reconstruction methods [38] make it possible to calculate the correlation functions and the string order. Thanks to the dipole power-law interaction in our model, we should find a power-law tail in the correlation functions in addition to the exponentially decay $C_{ij}^\alpha = Ae^{-\frac{|i-j|}{\xi}} + B|i-j|^{-a}$. By implementing a less time consuming method, we can calculate the entanglement spectrum of the ground state and determine whether it is double degenerate, according to the Haldane phase signature.

Robustness of the ground states to noise — Preparing the system in the Haldane phase is done adiabatically. Note that this can take more time than the time scale set by the noise sources. The main noise sources here are the fluctuating mag-

netic field in the z direction and the fluctuations in the Rabi frequencies of the driving fields. If during the path we represented above, the ground states are in the decoherence free subspace, the specific subspace of Hilbert space that is invariant under these fluctuations (to the first order), we will be able to walk on that path adiabatically.

The dressed basis used for representing the spins is the eigenstates of F_x $\{|u\rangle, |D\rangle, |d\rangle\}$. These states are robust to the magnetic noise in the z direction, as $\langle s | o_{(t)} F_z | s \rangle = 0$ for $|s\rangle \in \{|u\rangle, |D\rangle, |d\rangle\}$. Moreover, the ground state of the large D phase which is the topologically trivial state of $|D\rangle$ states in every site and the ground state of the Haldane phase [25, 26] which has the same number of sites occupied with $|u\rangle$ and $|d\rangle$ are robust to the fluctuations in the Rabi frequencies, as $o_{(t)} F_x |GS\rangle = o_{(t)} S_z |GS\rangle = 0$. The remarkable structure of the ground states explains why our model is decoupled from $H_{\text{res}} \propto S_z^i$ (Eq. 6), and we do not have to work hard to dynamically decouple it by a π -pulse sequence [39].

Higher Dimensions — We can also scale up to higher dimensions with more frustrated geometries of the quantum spin liquid phase where the interaction excitations are strong. Using the linear Paul trap, by lowering the transverse trap frequency ω_z enough, we observe a phase transition from the linear formation to a frustrated zigzag n-ladder formation [40]. As the fabrication technology progresses, arbitrary geometries could be produced for the ions lattice. The ground state of the spin liquid phase is characterized (and as a result can be detected) by the entanglement entropy that obeys the boundary law $S = a\sigma_R - \gamma$, where σ_R is the $d-1$ dimensional volume surrounding the region, and $\gamma = \log d$ is a fixed value in the topologically ordered phase, which is independent of the lattice's geometry [41–43].

Summary — We proposed a quantum simulation scheme for one-spin Heisenberg AFM systems. The Hamiltonian can be generated adiabatically, starting from the large D phase until it reaches the spin-liquid phase (or the Haldane phase in $d=1$). The ground states are robust to magnetic noise, decoupled from the fluctuations in the Rabi frequencies and can be detected by their characterization as mentioned above.

Acknowledgements — We thank E. Berg and D. Orgad for useful discussions and acknowledge the support of the European Commission (STREP EquaM).

-
- [1] R. P. Feynman, Int. J. Theor. Phys. **21**, 467 (1982).
 - [2] Iulia Buluta and Franco Nori, *Science* **326**, 108 (2009).
 - [3] Immanuel Bloch, Jean Dalibard and Sylvain Nascimbne, *Nature Physics* **8**, 267 (2012).
 - [4] D. Jaksch, C. Bruder, J. I. Cirac, C. W. Gardiner, and P. Zoller, *Phys. Rev. Lett.* **81**, 31083111 (1998).
 - [5] R. Blatt and C. F. Roos, *Nature Physics* **8**, 277 (2012).
 - [6] Michael J. Hartmann, Fernando G. S. L. Brando and Martin B. Plenio, *Nature Physics* **2**, 849 (2006).
 - [7] J. Cho, D. G. Angelakis, and S Bose, *Phys. Rev. A* **78**, 062338 (2008).

- [8] Z. X. Chen, Z. W. Zhou, X. Zhou, X. F. Zhou, and G. C. Guo, *Phys. Rev. A* **81**, 022303 (2010).
- [9] M. Neeley *et al.*, **325**, (5941): 722-725 (2009).
- [10] A. A. Guzik and P. Walther, *Nature Physics* **8**, 285291 (2012).
- [11] J. Simon *et al.*, *Nature* **474**, 307-312 (2011).
- [12] K. R. K. Rao, T. S. Mahesh, and A. Kumar *arXiv:1307.5220* (2013).
- [13] J. Struck *et al.*, *Science* **333**, 996 (2011).
- [14] X. S. Ma, B. Dakic, W. Naylor, A. Zeilinger, and P. Walther, *Nature Physics* **7**, 399405 (2011).
- [15] M. Johanning *et al.*, *J. Phys. B: At. Mol. Opt. Phys.* **42** (2009)
- [16] Ch. Schneider, *et al.*, *Reports on Progress in Physics*, **75**, 024401, (2012).
- [17] D. Porras and J. I. Cirac, *Phys. Rev. Lett.* **92**, 207901 (2004).
- [18] F. Mintert and C. Wunderlich *Phys. Rev. Lett.* **87**, 257904 (2001).
- [19] A. Friedenauer, H. Schmitz, J. T. Glueckert, D. Porras and T. Schaetz, *Nature Physics* **4**, 757 (2008).
- [20] E. E. Edwards *et al.*, *Phys. Rev. B* **82**, 060412 (2010).
- [21] R. Islam, *et al.*, *Science* **340**, 6132 (2013).
- [22] S. Zippilli, M. Johanning, S. M. Giampaolo, Ch. Wunderlich, and F. Illuminati, *arXiv:1304.0261* (2013).
- [23] J. W. Britton *et al.*, *Nature* **484**, 489492 (2012).
- [24] F. D. M. Haldane, *Phys. Rev. Lett.* **50**, 1153 (1983).
- [25] T. Kennedy and H. Tasaki, *Phys. Rev. B* **45**, 304 (1992).
- [26] T. Kennedy and H. Tasaki, *Commun. Math. Phys.* **147**, 431 (1992).
- [27] F. Pollmann, A. M. Turner, E. Berg, and M. Oshikawa, *Phys. Rev. B* **81**, 064439 (2010).
- [28] F. Pollmann, E. Berg, A. M. Turner, and M. Oshikawa, *Phys. Rev. B* **85**, 075125 (2012).
- [29] S. R. White, *Phys. Rev. B* **48**, 10345 (1993).
- [30] M. Kenzelmann *et al.*, *Phys. Rev. B* **66**, 024407 (2002).
- [31] D.F.V. James, *Appl. Phys. B* **66**, 181-190 (1998).
- [32] A. Bermudez *et al.*, *Phys. Rev. Lett.* **107**, 207209 (2011).
- [33] N. Timoney *et al.*, *Nature* **476**, 185 (2011).
- [34] S. C. Webster *et al.*, *arXiv 1303.3798* (2013).
- [35] M. Johanning *et al.*, *Phys. Rev. Lett.* **102**, 073004 (2009).
- [36] S. Sachdev, *Quantum Phase Transitions* (Cambridge University Press, Cambridge, 1999)
- [37] H. Li, and F. D. M. Haldane, *Phys. Rev. Lett.* **101**, 010504 (2008).
- [38] T. Baumgratz, D. Gross, M. Cramer, and M. B. Plenio, *Phys. Rev. Lett.* **111**, 020401 (2013).
- [39] L. Viola, E. Knill, and S. Lloyd, *Phys. Rev. Lett.* **82**, 2417 (1999).
- [40] R. C. Sterling *et al.*, *arXiv 1302.3781* (2013).
- [41] G. Vidal, J. I. Latorre, E. Rico, and A. Kitaev, *Phys. Rev. Lett.* **90**, 227902 (2003).
- [42] Y. Zhang, T. Grover, and A. Vishwanath, *Phys. Rev. B* **84**, 075128 (2011).
- [43] Y. Zhang, T. Grover, and A. Vishwanath, *Phys. Rev. Lett.* **107**, 067202 (2011).